IV. GRAVITY MEASUREMENT

By Kiyokazu Nishimura and Fumitoshi Murakami

Proceedure

Gravity measurement was carried out by surface ship gravity meter, Air-Sea Gravity Meter of La Coste and Romberg Co. The measured gravity values were correlated with the gravity value on land at Funabashi private pier (Chiba Prefecture). The absolute gravity value at this point is 979,802.9 mgal.

In the gravity measurements, the position of the ship is fixed by the NNSS (Navy Navigarion Satellite System) which uses the dead-reckoning regulation based on the satellite fix. The EM log was mainly used as the velocity sensor and sometimes the Doppler Sornor was used.

Gravity and other geophysical data were recorded at 30 sec. intervals on magnetic tape of the data acquisition system of the NNSS. The recorded data were compiled by the off-line system, and were recalculated about the position (including post-analysis). The data finally obtained was compiled in the data list, profiles and contour maps.

An example of the data list which contains free air anomalies "F-A A" and Bouguer anomalies "BA" with time (GMT), latitude, longitude and others is shown in Table

Table IV-1 An example of gravity data list.
DAY: Julian day, TIME: Hour and minute, SPD: speed of ship (knot), HDG: Heading of ship (degree), FREE AIR: Free air anomaly (mgal), DEPTH: Water depth (m), MAGT: Total magnetic force (gamma), ANOM: Magnetic anomaly reduced from IGRF (gamma).

DAY	TIME	LATITUDE	LONGITUDE	SPD	HDG	FREE AIR	F-A A	B A	DEPTH	MAGT	ANOM
121	0	38 40.3 N	142 20.1 E	11.6	89.	980162.7	99.7	130.7	763.	46798.	-93.
121	5	38 40.3 N	142 21.3 E	11.4	89.	163.0	99.9	130.9	762.	46784.	-101.
121	10	38 40.4 N	142 22.5 E	11.5	89.	161.4	98.2	129.6	772.	46770.	-109.
121	15	38 40.4 N	142 23.7 E	11.4	89.	155.6	92.5	125.8	820.	46788.	-85.
121	20	38 40.4 N	142 24.9 E	11.4	89.	148.6	85.4	121.6	890.	46776.	-91.
121	25	38 40.4 N	142 26.1 E	11.6	89.	143.9	80.7	120.1	970.	46782.	-79.
121	30	38 40.4 N	142 27.3 E	11.3	89.	133.7	70.5	113.2	1050.	46792.	-64.
121	35	38 40.4 N	142 28.6 E	11.3	89.	126.1	62.8	108.2	1115.	46798.	-52.
121	40	38 40.5 N	142 29.8 E	11.4	89.	123.0	59.7	106.5	1150.	46798.	-46.
121	45	38 40.5 N	142 31.0 E	11.4	90.	117.3	54.0	101.6	1170.	46795.	-43.
121	50	38 40.5 N	142 32.2 E	11.6	89.	114.9	51.6	99.6	1180.	46790.	-42.
121	55	38 40.4 N	142 33.5 E	11.6	93.	114.3	51.1	99.8	1200.	46777.	-48.
121	100	38 40.4 N	142 34.7 E	11.4	94.	112.4	49.3	99.1	1225.	46760.	-58.
121	105	38 40.3 N	142 35.9 E	11.3	94.	112.2	49.2	100.6	1265.	46768.	-44.
121	110	38 40.2 N	142 37.1 E	11.4	94.	112.4	49.4	101.3	1275.	46766.	-39.
121	115	38 40.2 N	142 38.3 E	11.5	94.	109.0	46.2	98.2	1280.	46770.	-28.
121	120	38 40.1 N	142 39.5 E	11.4	94.	105.0	42.3	94.5	1285.	46769.	-22.
121	125	38 40.0 N	142 40.7 E	11.6	94.	102.0	39.4	92.3	1300.	46758.	-27.
121	130	38 40.0 N	142 42.0 E	11.5	94.	97.2	34.7	88.3	1320.	46747.	-31.
121	135	38 39.9 N	142 43.2 E	11.5	94.	92.4	29.9	84.4	1340.	46746.	-25.
121	140	38 39.9 N	142 44.4 E	11.5	92.	84.7	22.3	77.2	1350.	46718.	-47.
121	145	38 39.8 N	142 45.6 E	11.7	91.	79.8	17.4	73.1	1370.	46697.	-61.
121	150	38 39.8 N	142 46.9 E	11.3	91.	71.7	9.4	66.3	1400.	46685.	-67.
121	155	38 39.8 N	142 48.1 E	11.5	91.	67.1	4.8	63.8	1450.	46668.	-78.
121	200	38 39.8 N	142 49.3 E	11.5	91.	63.4	1.1	60.9	1470.	46653.	-86.
121	205	38 39.8 N	142 50.5 E	11.2	85.	59.3	-2.9	57.6	1490.	46636.	-98.
121	210	38 39.9 N	142 51.7 E	11.3	89.	55.6	-6.8	55.0	1520.	46628.	-100.

IV-1. The Gravity contour maps are drawn with respect of the free air and Bouguer anomalies, and are shown in Fig. IV-1 and Fig. IV-2. In the Bouguer anomaly contour map, the anomalies are calculated assuming a Bouguer correction density of 2.0 gr/cm^3, and water density of 1.03 gr/cm^3. Topographic correction is not calculated.

The profiles are shown with respect of the free air anomalies (FA) and the Bouguer anomalies (BA, BA′) with the magnetic anomalies (MG) and the topography (TP). In the topography profiles, the vertical scale is ten times as long as the horizontal scale. The Bouguer anomalies in the profiles are drawn up for two cases; one is calculated from the Bouguer correction density of 2.0 gr/cm^3 (BA), and the other is calculated from the Bouguer correction density of 2.67 gr/cm^3 (BA′). These two corrections are used in conjunction with the two dimensional topographic corrections. The method of TALWANI *et al.* (1959) was used in the topographic correction. West or north is indicated on the left side of all the profiles.

On each contour map, the range of the enclosed four points 39°55′N 142°0′E, 41°30′N 141°30′E, 41°30′N 143°50′E, 39°55′N 145°40′E, (east from Hachinohe), survey lines of L20–L26, were affected by gravity meter trouble in that the heater in the sensor of the gravity meter did not operate under normal condition. Consequently, the gravity values in the region increased. The erroneous gravity values are compared with the values of the surveyed line of L46 which crosses all of the lines failing to leave correct data, and with the neighboring lines to check the smooth connections. The data are also compared with other data taken by other cruises. Consequentry, the erroneous gravity data are found to always exceed 40 mgal as compared with that of the correct one. The erroneous range is indicated by the broken dotted line which are reduced from 40 mgal from the obtained values. In the same manner, the free air and Bouguer anomalies in profiles L20–L26 are indicated to reduce 40 mgal to the measured values.

Results

Free air anomalies

Low gravity anomalies are observed along the Kulile Trench and Japan Trench. The axis of these low anomalies extend northeast to southwest along the Kulile Trench, bend in the vicinity of 41°15′E 144°50′E (southeast of Cape Erimo), and extend north-northeast to south-southwest.

High anomalies are observed along the coastal region of east Hokkaido to the northeast and along the Sanriku coast.

The center of low anomaly in the northeast (about 200 km) from Etorofu Island is calculated to approximately −300 mgal. The center of the anomaly lies about 12 km from the topographic trench axis toward the land.

On the continental slope off the eastern end of Hokkaido to near Shikotan Island, the gravity gradient is steep (profiles L36–L45), it increases at the rate of 10 mgal/km to the south-east.

The center of the high anomaly southeast of Etorofu Island is calculated as approximately 220 mgal. This region is considered to be on the extention of the islands from Nemuro Peninsula and Shikotan Island. The anomaly may be caused by the tectonic high of the Cretaceous rocks.

The high anomaly of 160 mgal is distributed along the northeastern coast of Hokkaido. This anomaly corresponds to the southern ridge of high gravity anomaly of 230 mgal at Nemuro (Geographical Survey Institute, 1955) which is the one of the highest values in Japan.

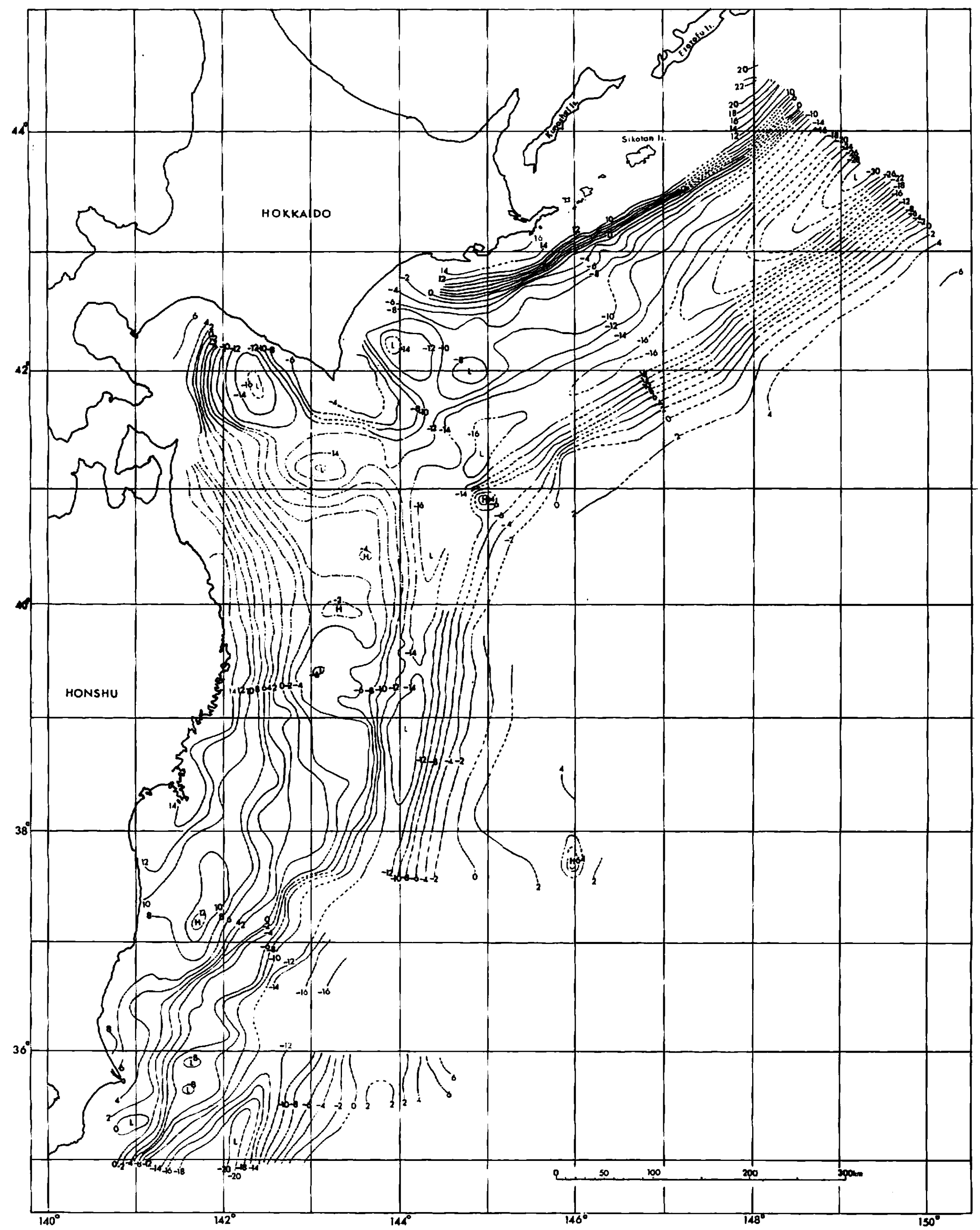

Fig. IV-1 The contour map of the free air anomalies off Northeast Japan and Hokkaido. The number in contours are in units of 10 mgal, and contour interval is 20 mgal.

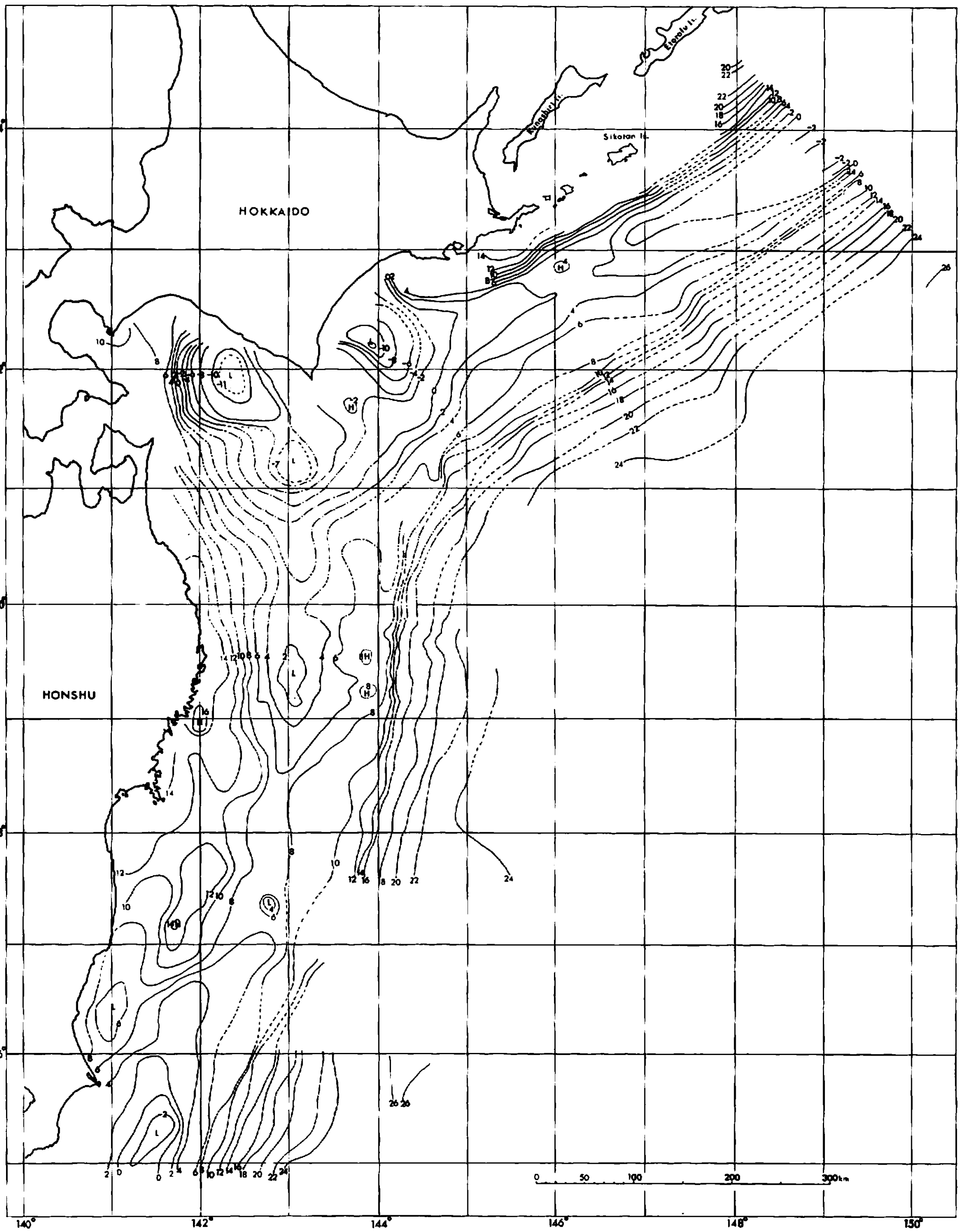

Fig. IV-2 The contour map of the Bouguer anomalies off Northeast Japan and Hokkaido. 2.0 gr/cm³ for the subbottom density and 1.03 gr/cm³ for the water density are used for the Bouguer correction. The number in contours are in units of 10 mgal, and contour interval is 20 mgal.

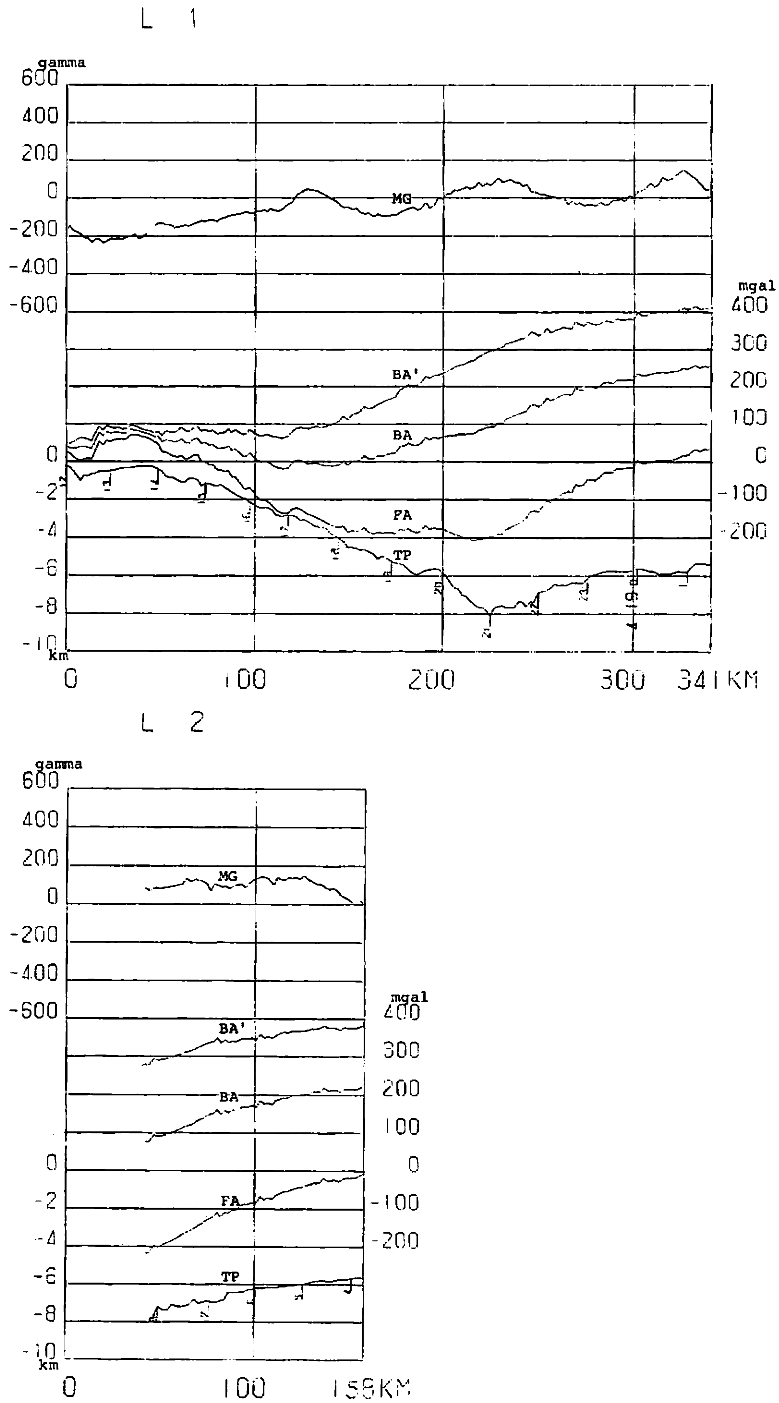

(A)

Fig. IV-3 Profiles of topography and anomalies.
TP: topography, FA: Free air anomalies, BA: Bouguer anomalies (Bouguer correction density 2.0 gr/cm^3), BA′: Bouguer anomalies (Bouguer correction density 2.67 gr/cm^3), MG: Magnetic anomalies resulted by the reduction of IGRF. Time (JST) are drawn below profile of topography. Dates are drawn every 0 o'clock. In the profiles of the topography, vertical scale is ten times as long as horizontal scale.

L 3

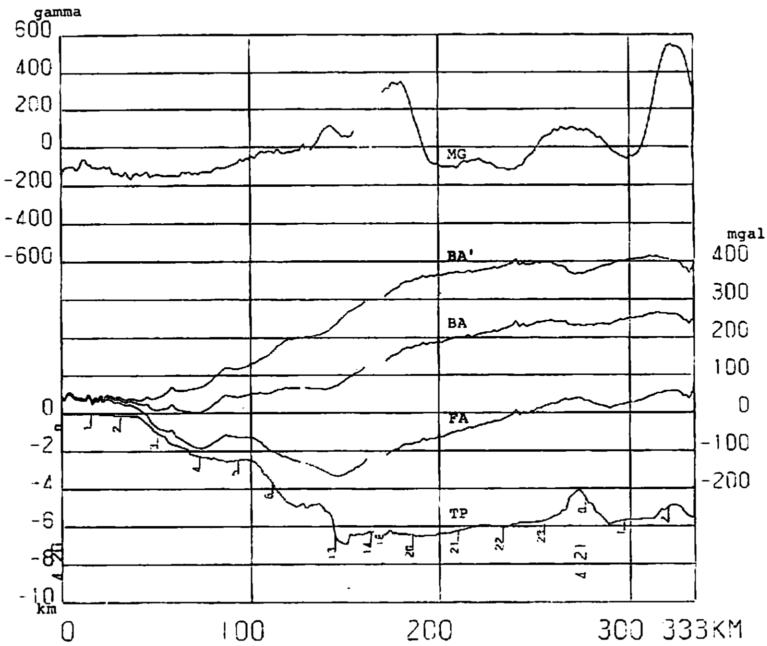
gamma
600
400
200
0
-200
-400
-600
MG
BA'
BA
FA
TP
mgal
400
300
200
100
0
-100
-200
0
-2
-4
-6
-8
-10
km
0
100
200
300 333KM

L 4

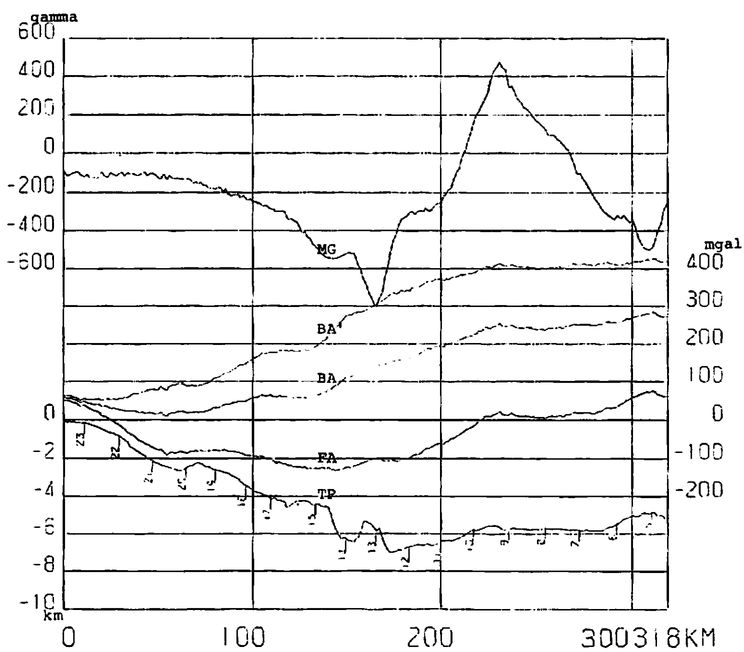
gamma
600
400
200
0
-200
-400
-600
MG
BA'
BA
FA
TP
mgal
400
300
200
100
0
-100
-200
0
-2
-4
-6
-8
-10
km
0
100
200
300318KM

(B)

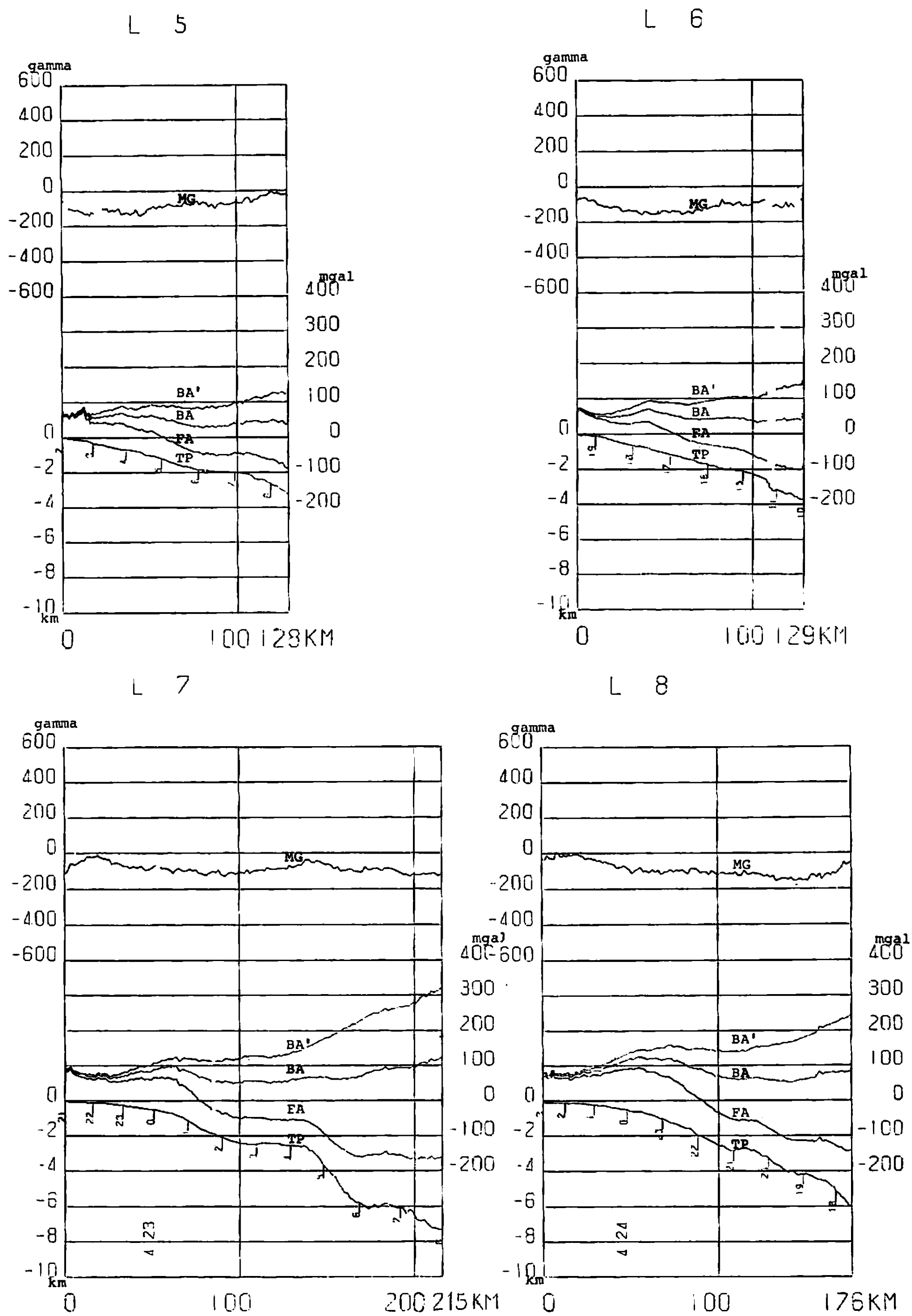
L 5
gamma
600
400
200
0
-200
-400
-600
mgal
400
300
200
100
0
-100
-200
MG
BA'
BA
FA
TP
0
-2
-4
-6
-8
-10
km
0
100 128KM
L 6
gamma
mgal
MG
BA'
BA
FA
TP
100 129KM
L 7
gamma
mgal
MG
BA'
BA
FA
TP
0
100
200 215KM
L 8
gamma
mgal
MG
BA'
BA
FA
TP
0
100
176KM

(C)

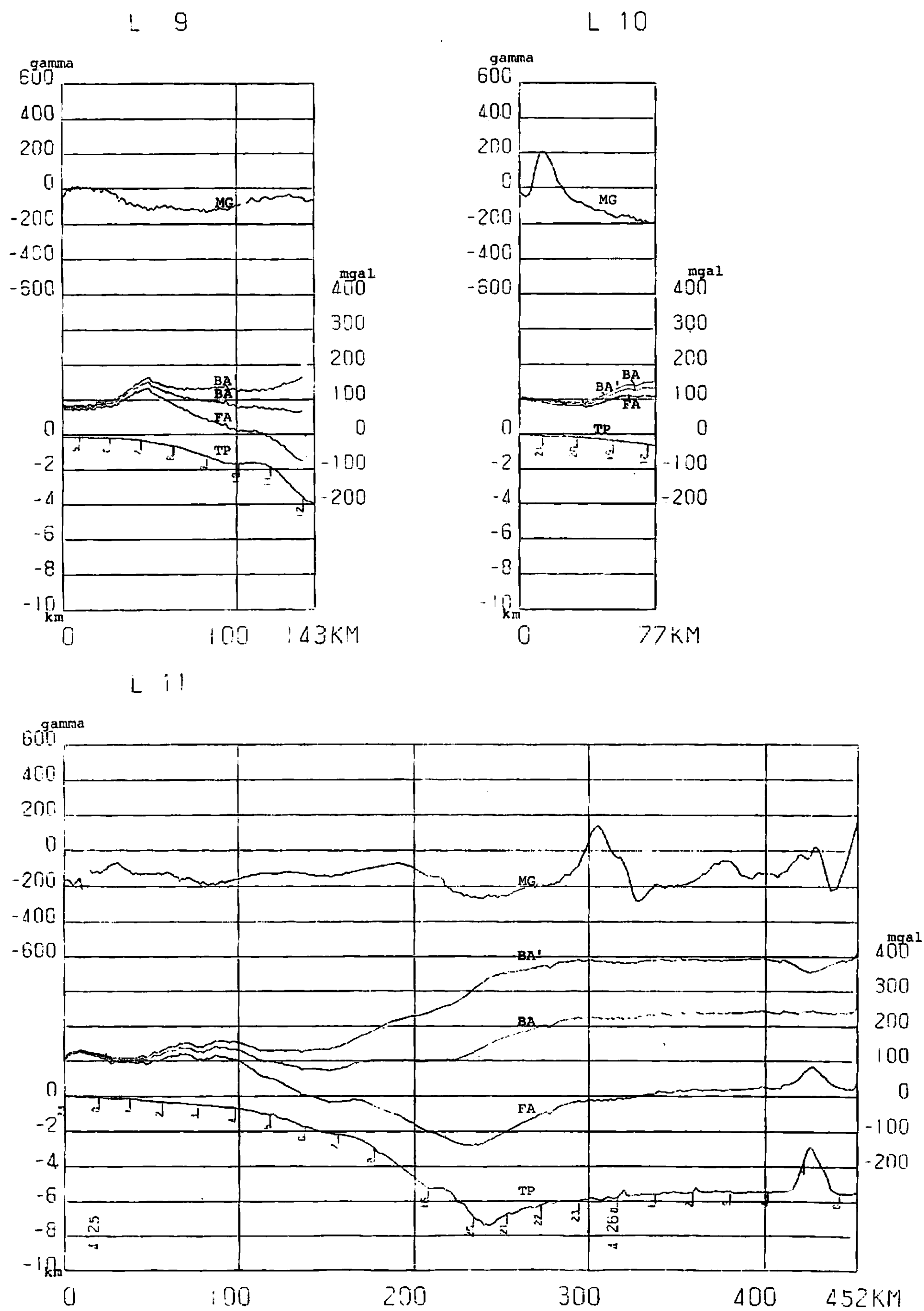

(D)

L 12

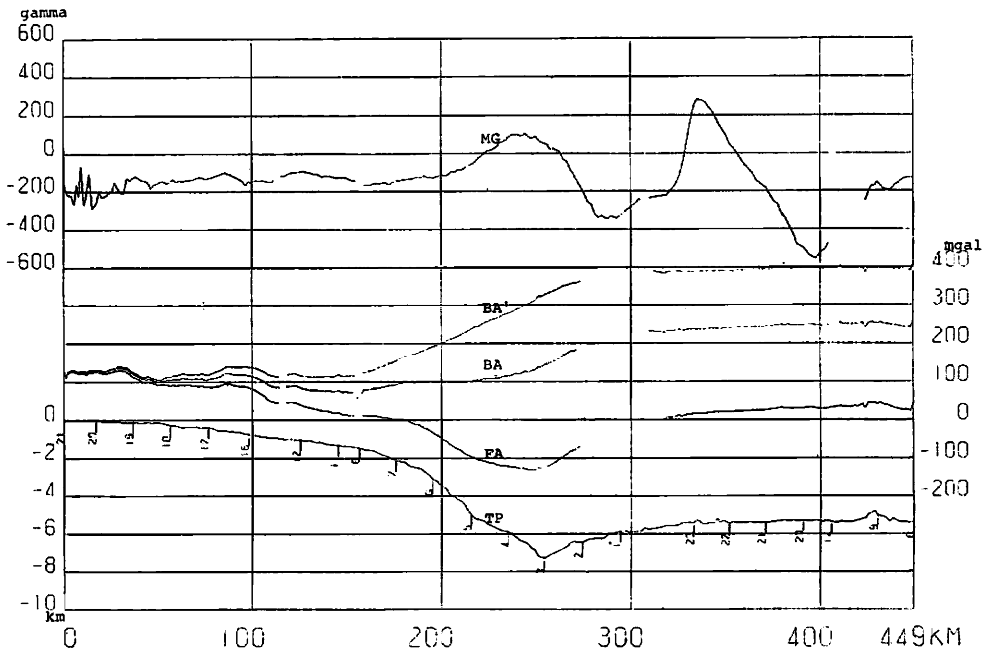
gamma
600
400
200
0
-200
-400
-600
MG
BA'
BA
FA
TP
mgal
400
300
200
100
0
-100
-200
0
-2
-4
-6
-8
-10
km
0
100
200
300
400
449KM

L 13

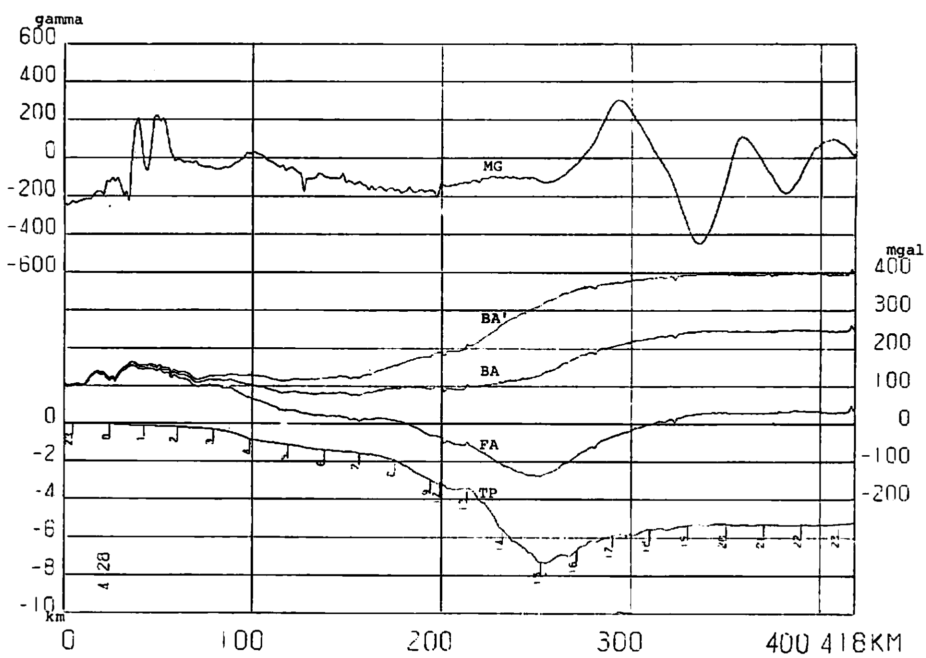
gamma
600
400
200
0
-200
-400
-600
MG
BA'
BA
FA
TP
mgal
400
300
200
100
0
-100
-200
0
-2
-4
-6
-8
-10
km
0
100
200
300
400 418KM

(E)

L 14

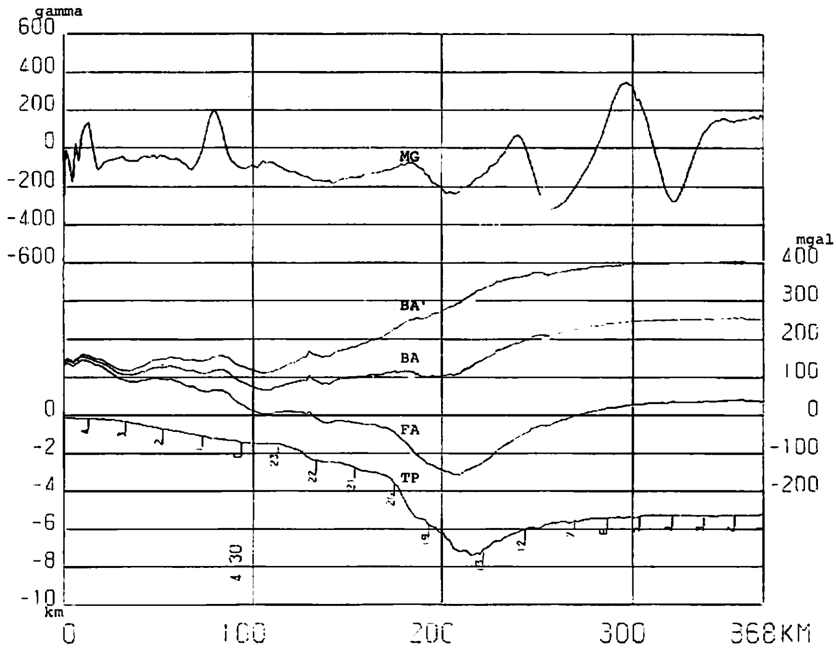
gamma
600
400
200
0
-200
-400
-600
MG
mgal
400
300
200
100
0
-100
-200
BA'
BA
FA
TP
0
-2
-4
-6
-8
-10
km
0
100
200
300
368KM

L 15

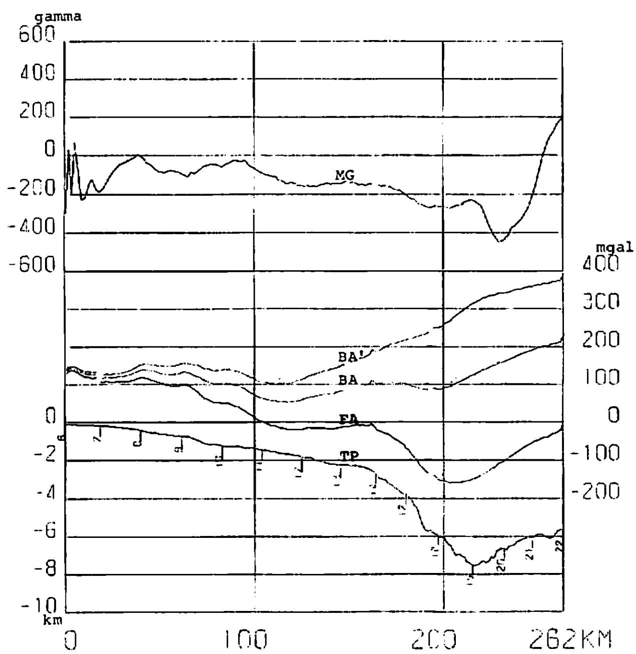
gamma
600
400
200
0
-200
-400
-600
MG
mgal
400
300
200
100
0
-100
-200
BA'
BA
FA
TP
0
-2
-4
-6
-8
-10
km
0
100
200
262KM

(F)

L 16

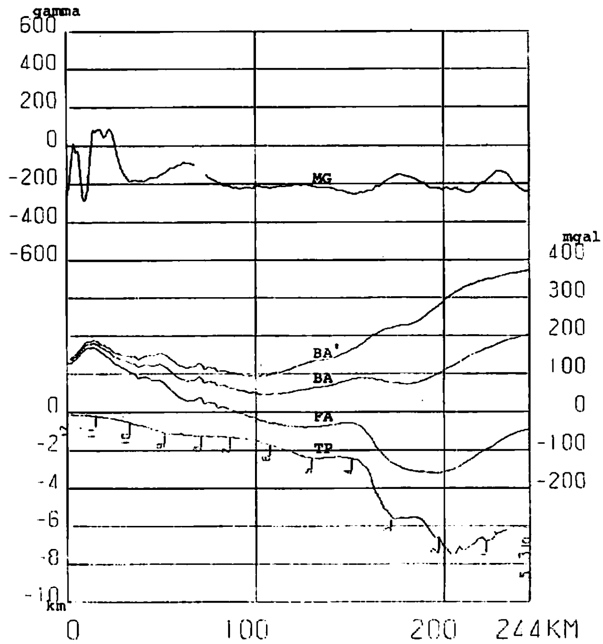
gamma
600
400
200
0
-200
-400
-600
MG
mgal
400
300
200
100
0
-100
-200
BA'
BA
FA
TP
0
-2
-4
-6
-8
-10
km
0
100
200
244KM

L 17

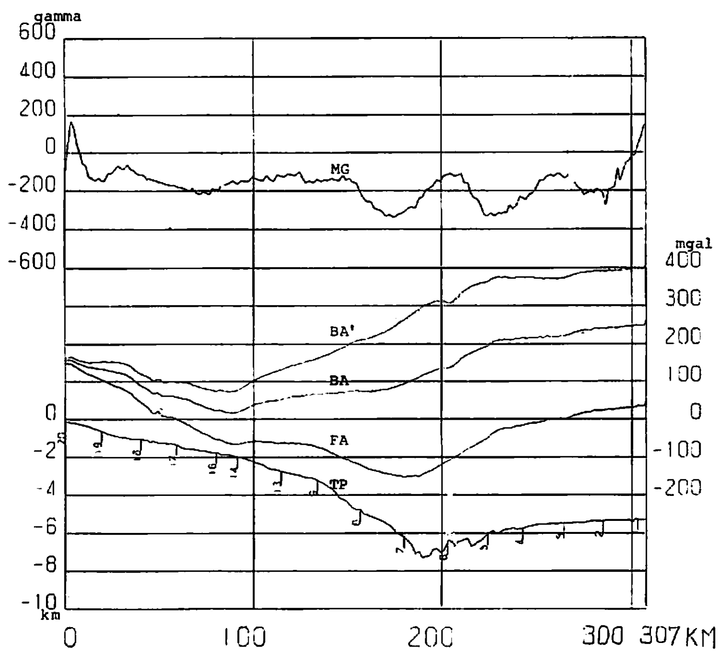
gamma
600
400
200
0
-200
-400
-600
MG
mgal
400
300
200
100
0
-100
-200
BA'
BA
FA
TP
0
-2
-4
-6
-8
-10
km
0
100
200
300
307KM

(G)

L 18

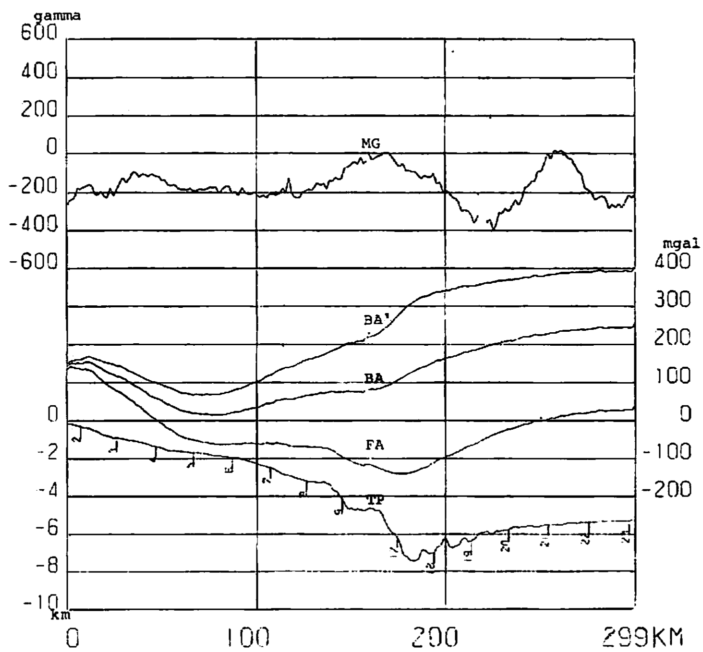
gamma
600
400
200
0
-200
-400
-600
MG
mgal
400
300
200
100
0
-100
-200
BA'
BA
FA
TP
0
-2
-4
-6
-8
-10
km
0
100
200
299KM

L 19

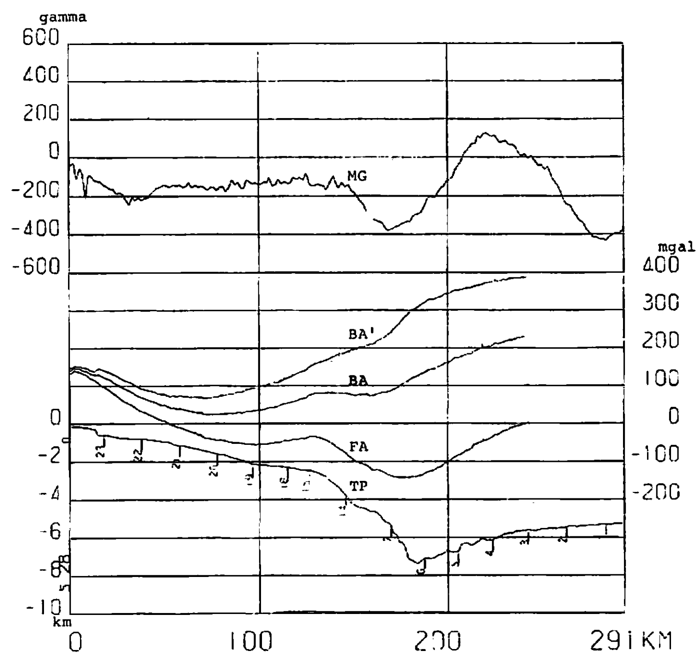
gamma
600
400
200
0
-200
-400
-600
MG
mgal
400
300
200
100
0
-100
-200
BA'
BA
FA
TP
0
-2
-4
-6
-8
-10
km
0
100
200
291KM

(H)

L 20

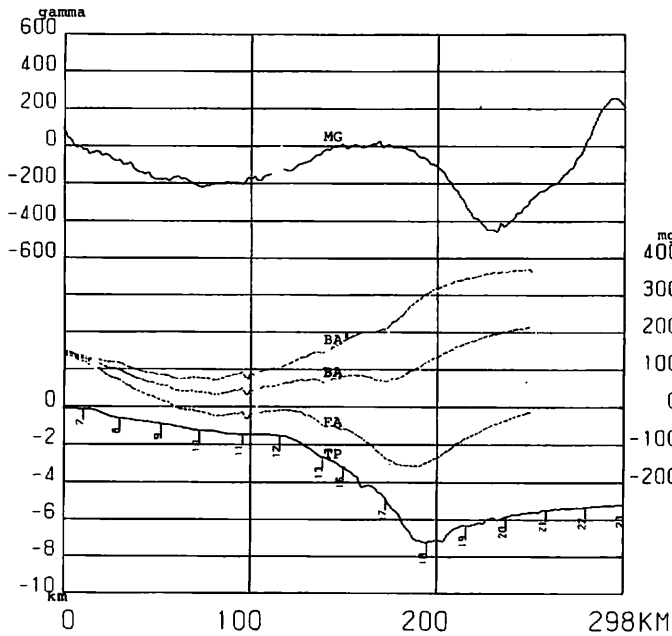
gamma
600
400
200
0
-200
-400
-600
MG
mgal
400
300
200
100
0
-100
-200
BA'
BA
FA
TP
0
-2
-4
-6
-8
-10
km
0
100
200
298KM

L 22

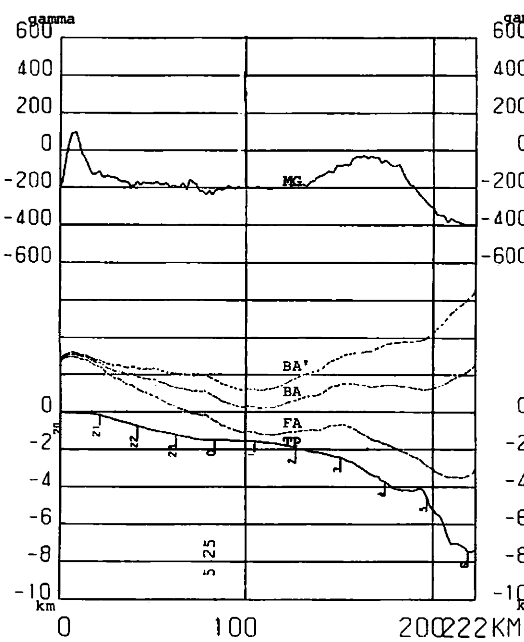
gamma
600
400
200
0
-200
-400
-600
MG
BA'
BA
FA
TP
0
-2
-4
-6
-8
-10
km
5 25
0
100
200
222KM

L 21

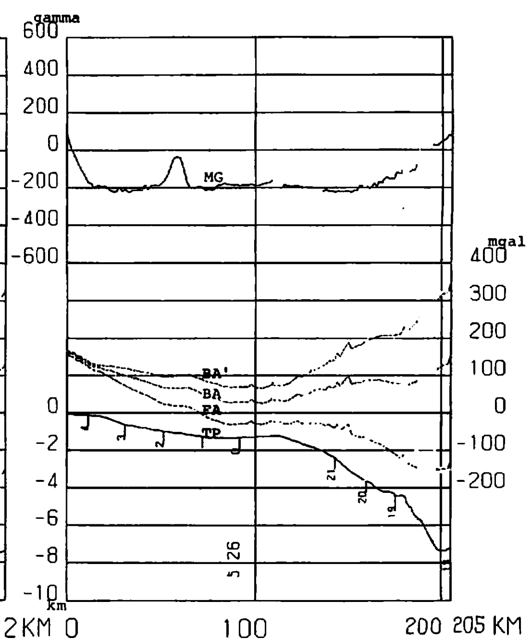
gamma
600
400
200
0
-200
-400
-600
MG
mgal
400
300
200
100
0
-100
-200
BA'
BA
FA
TP
0
-2
-4
-6
-8
-10
km
5 26
0
100
200
205 KM

(I)

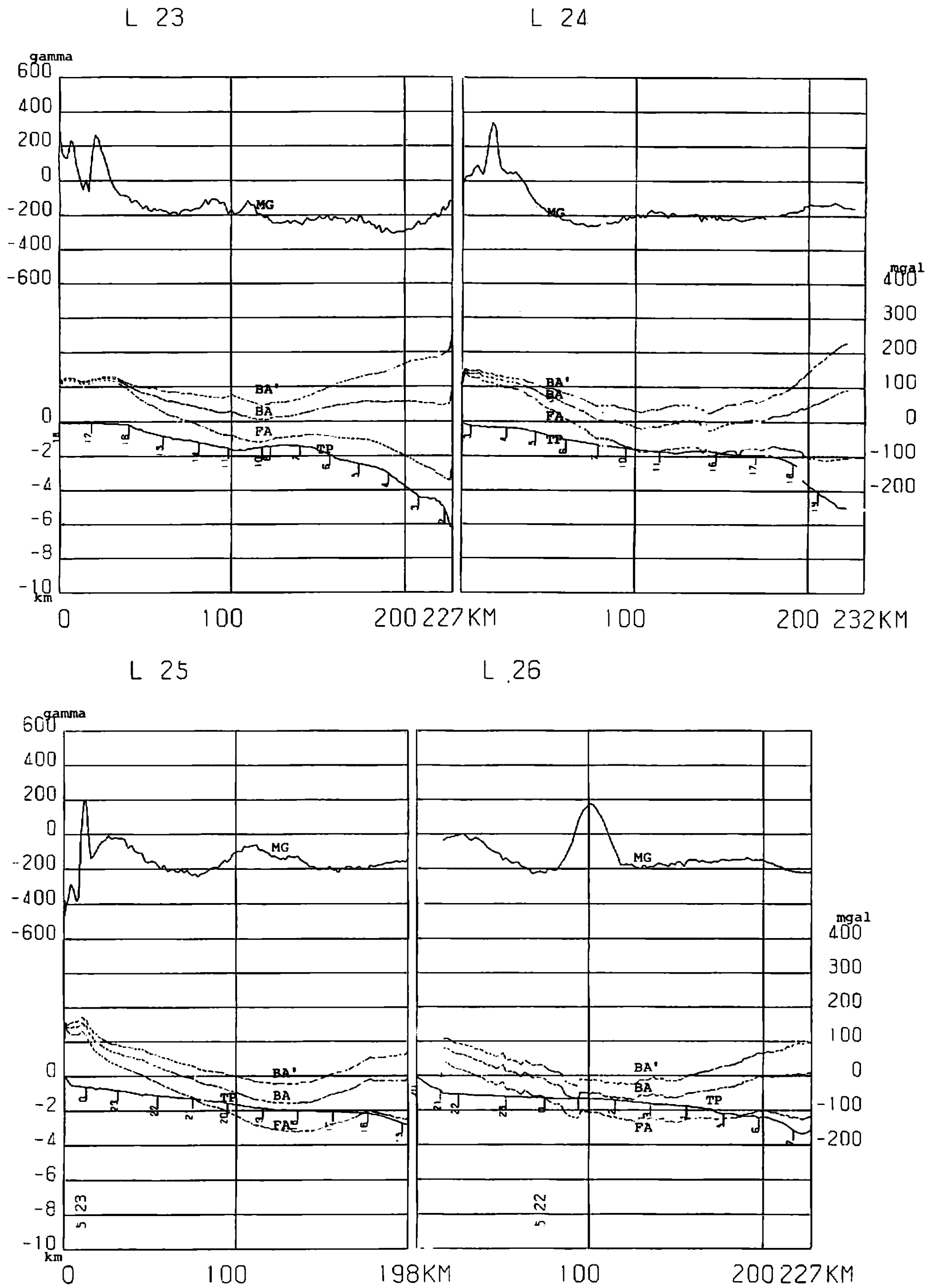

L 23
L 24
L 25
L 26
gamma
mgal
600
400
200
0
-200
-400
-600
300
100
-100
-2
-4
-6
-8
-10
km
MG
BA'
BA
FA
TP
0
100
200 227KM
200 232KM
198KM
200 227KM

(J)

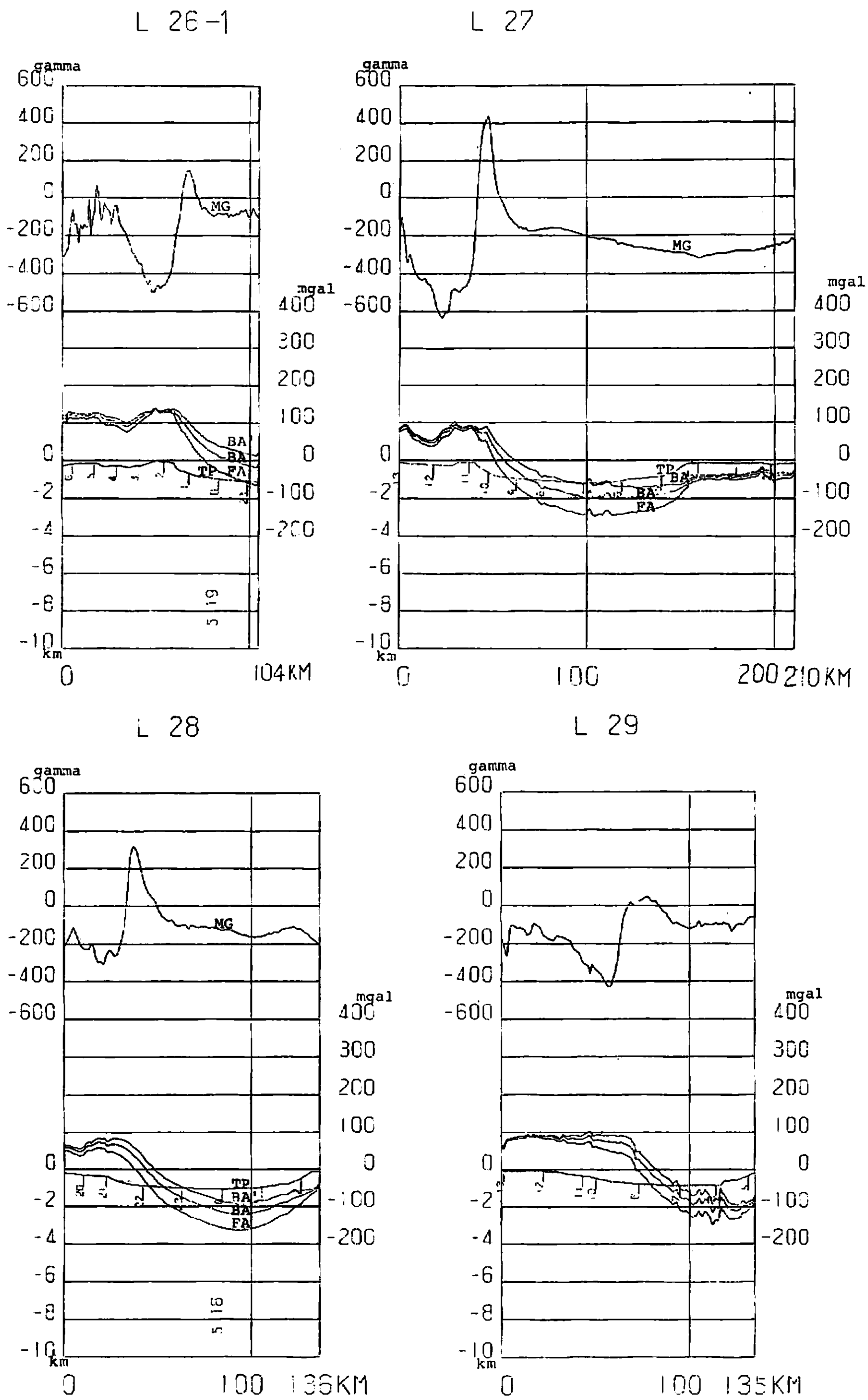
L 26-1
L 27
L 28
L 29
gamma
600
400
200
0
-200
-400
-600
mgal
400
300
200
100
0
-100
-200
-2
-4
-6
-8
-10
km
MG
BA
FA
TP
104KM
100
200 210KM
136KM
135KM

(K)

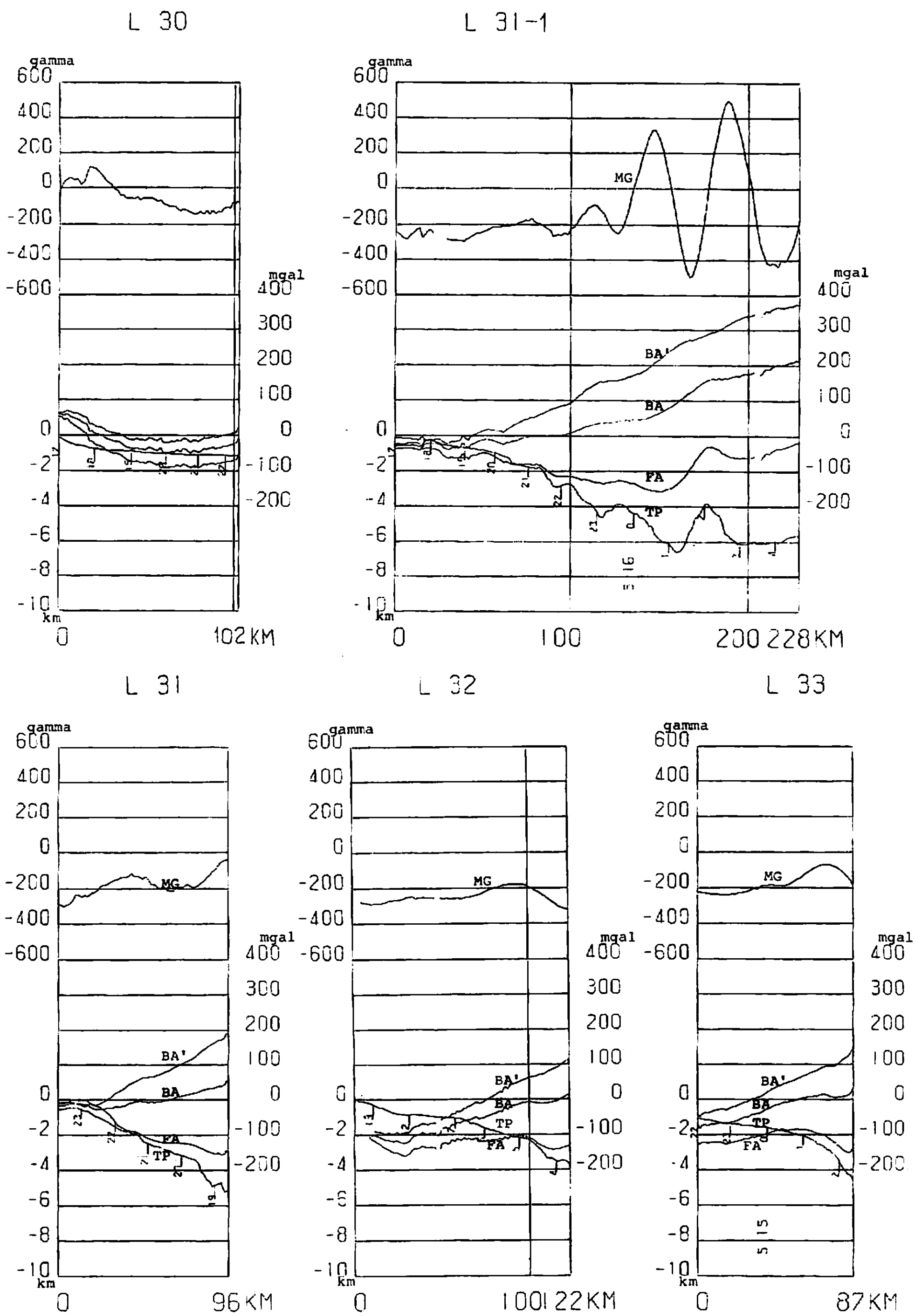
L 30
L 31-1
L 31
L 32
L 33
gamma
mgal
km
MG
BA'
BA
FA
TP
0
102KM
100
200 228KM
96KM
100 122KM
87KM

(L)

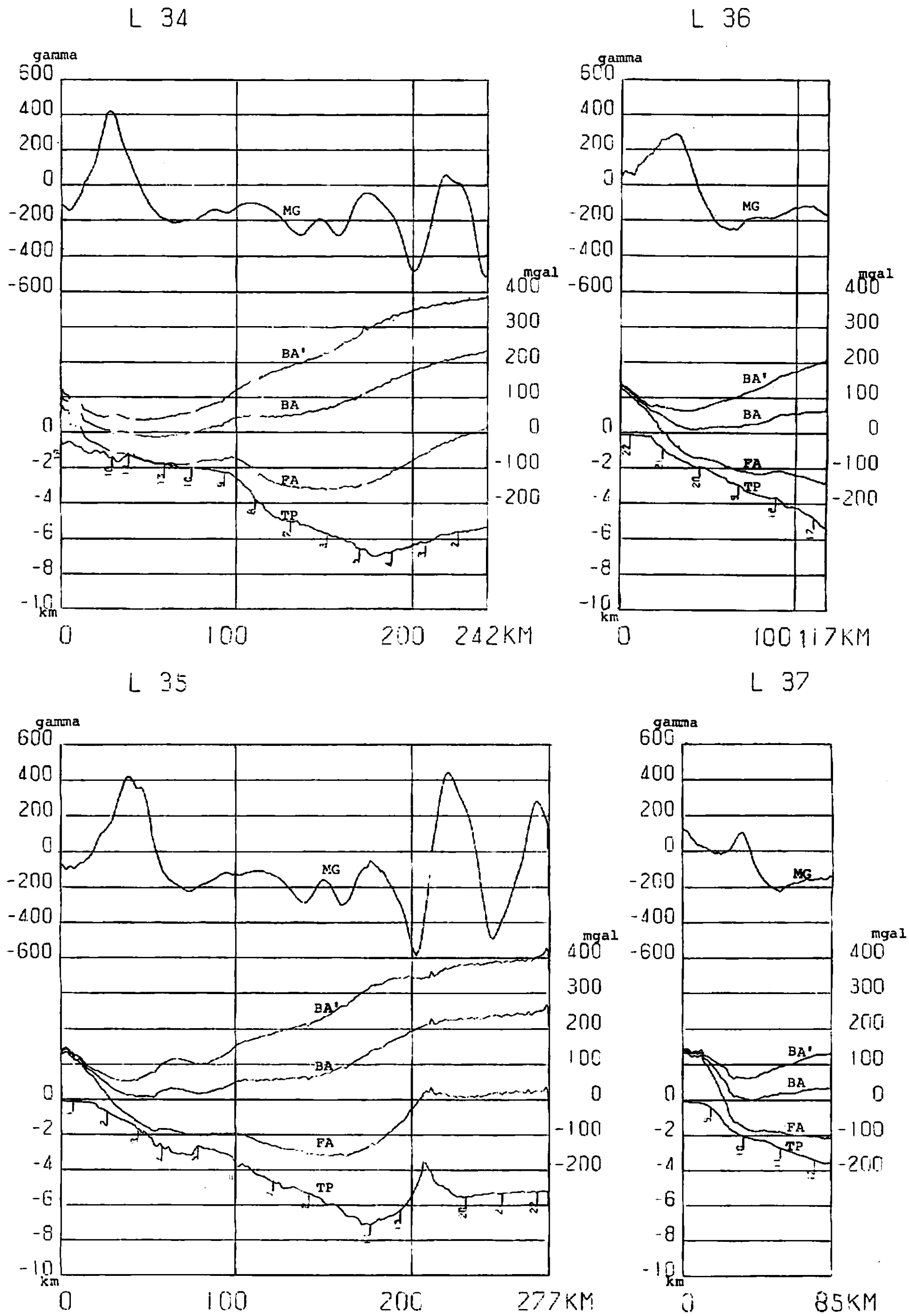
L 34
gamma
600
400
200
0
-200
-400
-600
MG
mgal
400
300
200
100
0
-100
-200
BA'
BA
FA
TP
0
-2
-4
-6
-8
-10
km
0
100
200
242KM
L 36
gamma
600
400
200
0
-200
-400
-600
MG
mgal
400
300
200
100
0
-100
-200
BA'
BA
FA
TP
0
-2
-4
-6
-8
-10
km
0
100
117KM
L 35
gamma
600
400
200
0
-200
-400
-600
MG
mgal
400
300
200
100
0
-100
-200
BA'
BA
FA
TP
0
-2
-4
-6
-8
-10
km
0
100
200
277KM
L 37
gamma
600
400
200
0
-200
-400
-600
MG
mgal
400
300
200
100
0
-100
-200
BA'
BA
FA
TP
0
-2
-4
-6
-8
-10
km
0
85KM

(M)

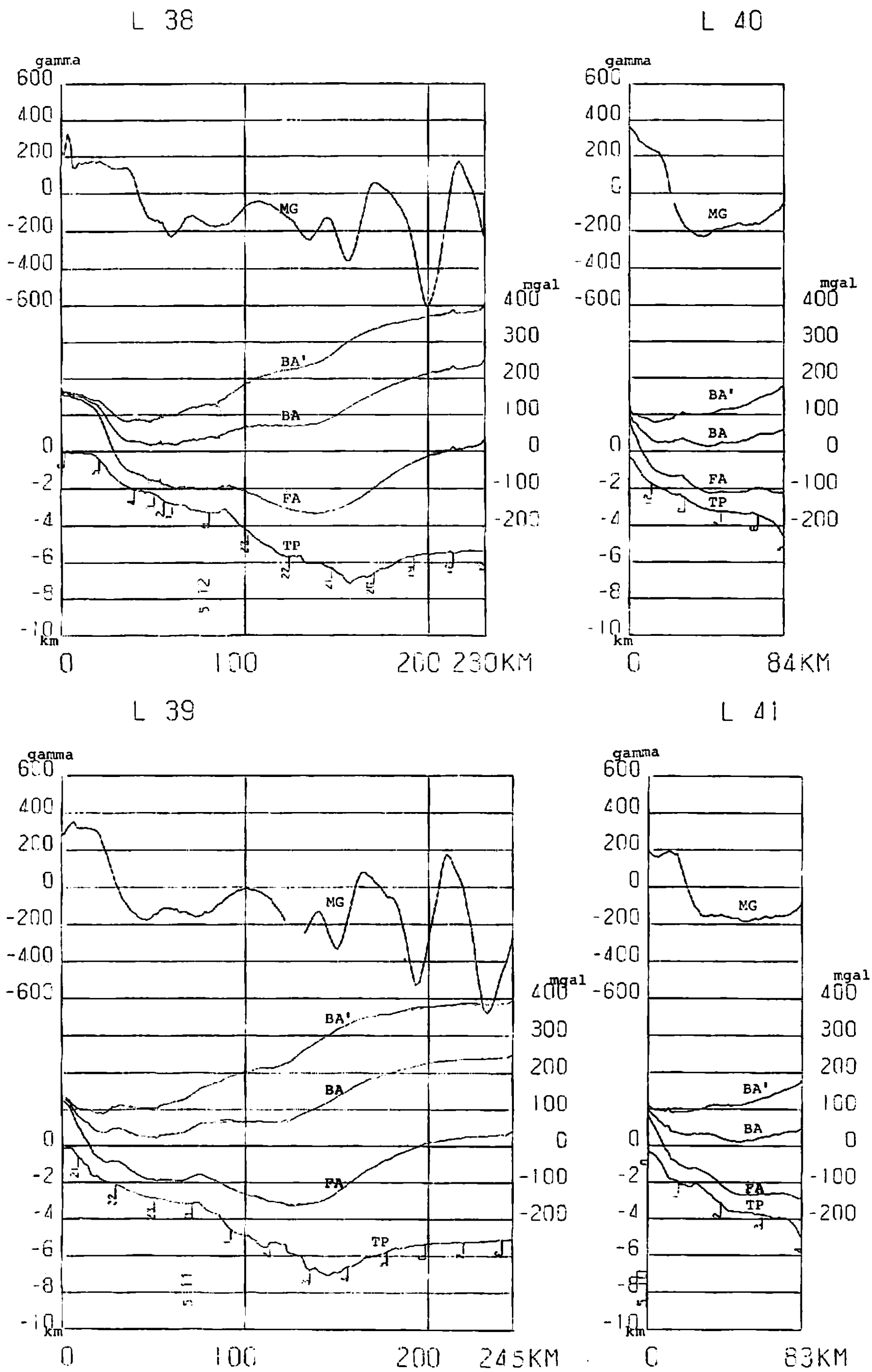
L 38
gamma
600
400
200
0
-200
-400
-600
mgal
400
300
200
100
0
-100
-200
MG
BA'
BA
FA
TP
0
-2
-4
-6
-8
-10
km
0
100
200 230KM
L 40
gamma
600
400
200
-200
-400
-600
mgal
400
300
200
100
0
-100
-200
MG
BA'
BA
FA
TP
0
-2
-4
-6
-8
-10
km
0
84KM
L 39
gamma
600
400
200
0
-200
-400
-600
mgal
400
300
200
100
0
-100
-200
MG
BA'
BA
FA
TP
0
-2
-4
-6
-8
-10
km
0
100
200
245KM
L 41
gamma
600
400
200
0
-200
-400
-600
mgal
400
300
200
100
0
-100
-200
MG
BA'
BA
FA
TP
0
-2
-4
-6
-8
-10
km
83KM

(N)

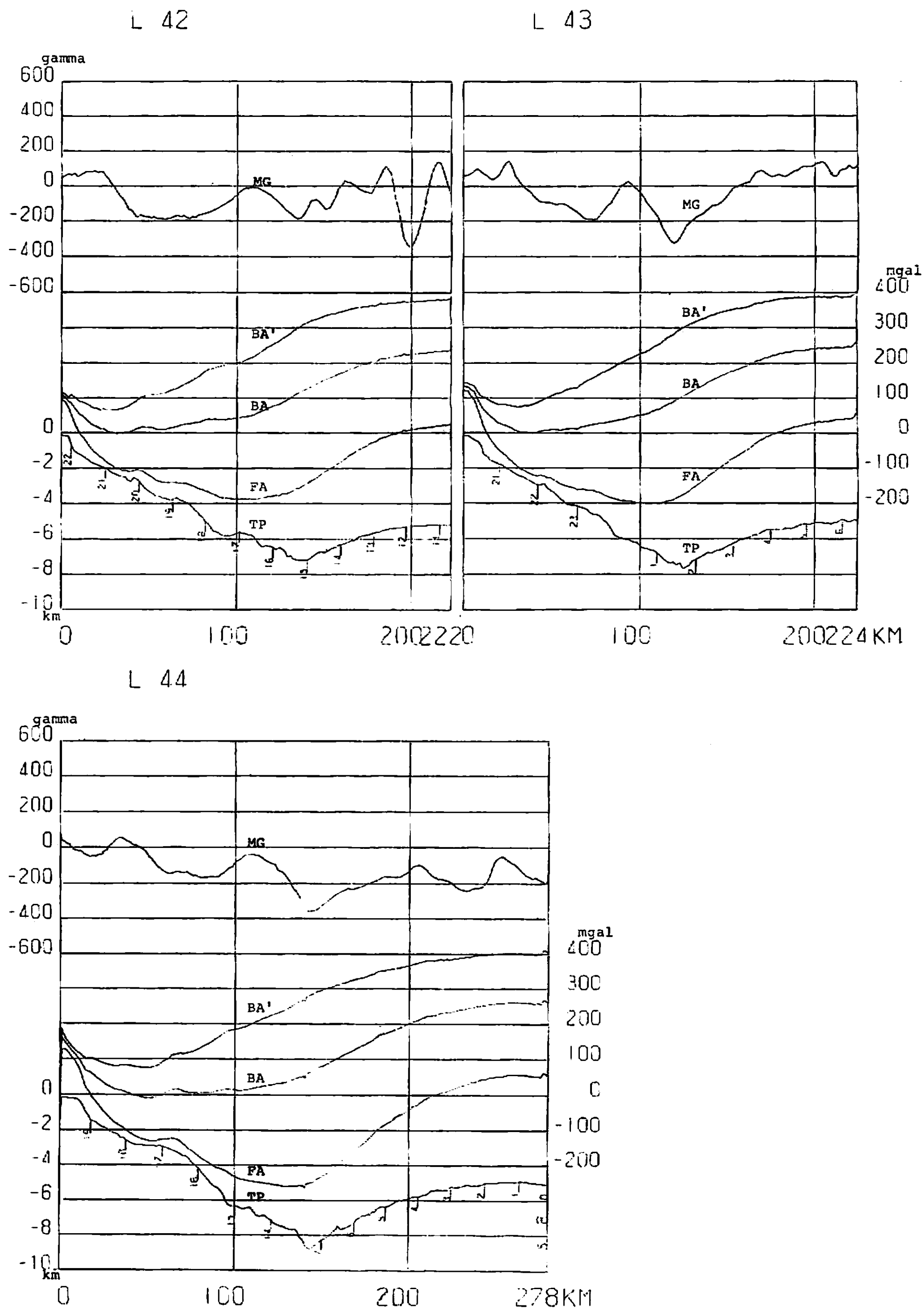
L 42
L 43
L 44
gamma
600
400
200
0
-200
-400
-600
mgal
400
300
200
100
0
-100
-200
MG
BA'
BA
FA
TP
0
-2
-4
-6
-8
-10
km
0
100
200222
0
100
200224KM
278KM

(O)

L 45

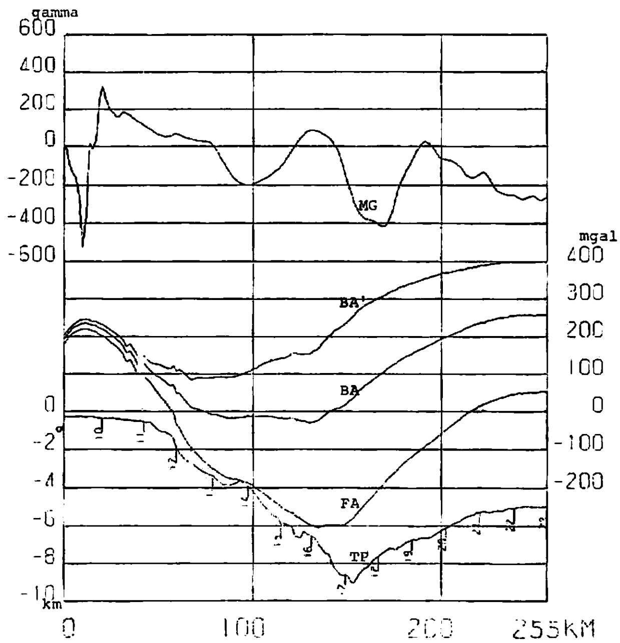

L 46-a

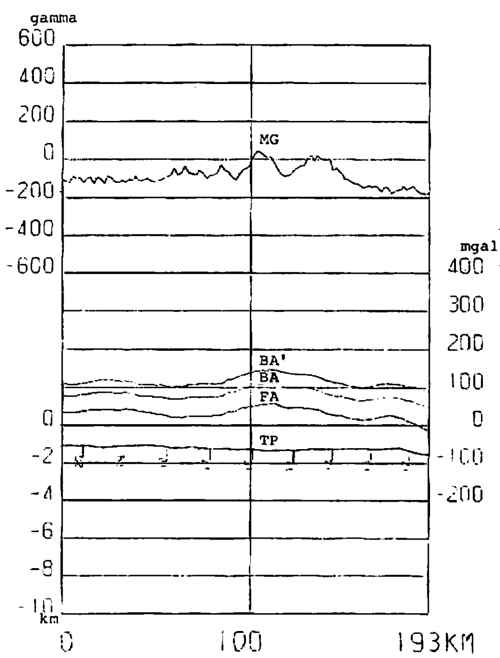

L 46-b

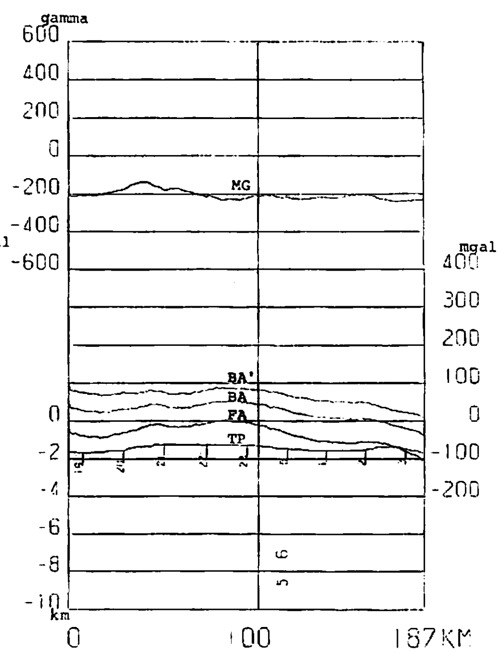

(P)

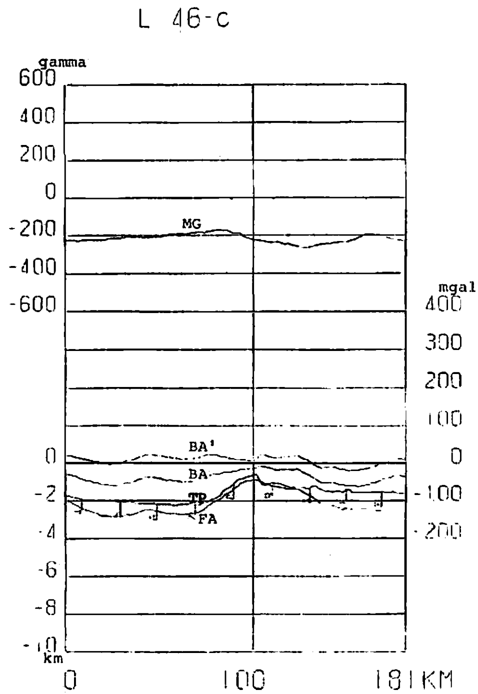
L 46-c
gamma
600
400
200
0
-200
-400
-600
MG
mgal
400
300
200
100
0
-100
-200
BA'
BA
TP
FA
0
-2
-4
-6
-8
-10
km
0
100
181KM

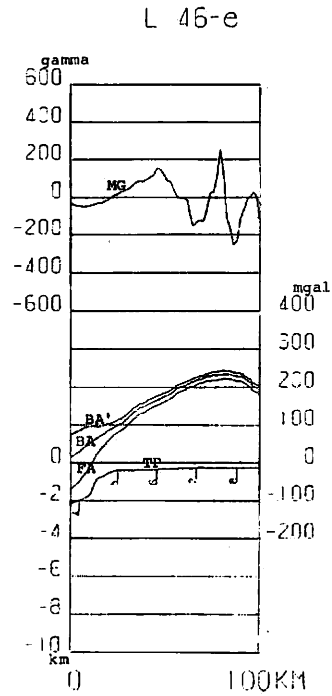
L 46-e
gamma
600
400
200
0
-200
-400
-600
MG
mgal
400
300
200
100
0
-100
-200
BA'
BA
FA
TP
0
-2
-4
-6
-8
-10
km
0
100KM

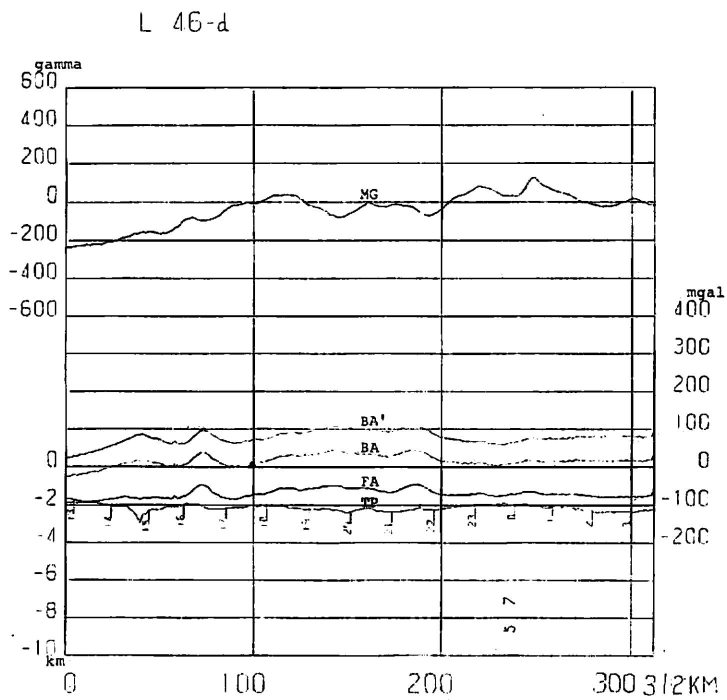
L 46-d
gamma
600
400
200
0
-200
-400
-600
MG
mgal
400
300
200
100
0
-100
-200
BA'
BA
FA
TP
0
-2
-4
-6
-8
-10
km
0
100
200
300
312KM

(Q)

The axis of the minimum free air anomalies corresponds to the trench which does not agree with the topographic trench axis, and exists on the slope of the trench a little to the land-ward side. From the differences of each survey line across the trench, the axis of the minimum free air anomalies in the Kurile Trench lies approximately 12–28 km (an average distance of 19 km) from the topographic trench axis towards land (to the northwest).

The center of the low anomaly at the junction of the two trenches southeast of Cape Erimo is calculated as approximately −160 mgal. The high anomaly of −30 mgal exists above the Erimo seamount to the south of the above mentioned low anomaly region. According to profile L31–1, the high anomaly exceeds 130 mgal as compared with that in the trench region.

Two low anomalies are observed in the Hidaka Basin. The anomaly is approximately −160 mgal in the northern part and approximately −160 mgal in the southern part. One more low anomaly is observed to the east of Cape Erimo where the anomaly exceeds −140 mgal.

The high anomalies of 140 mgal exist along the Sanriku coast, and the center of these high anomalies exists along the east coast of the Kitakami Mountains on land.

The axis of the free air anomalies in the Japan Trench lies approximately 6–9 km (an average distance of 7 km) from the topographic trench axis towards the land (to the west). The Japan Trench is similar to the Kurile Trench from the view point of the anomaly shift towards land, but the amount of the shift in the Japan Trench is smaller than in the Kurile Trench.

The low anomaly along the Japan Trench is approximately −140 mgal and is smaller in comparison with that in the Kurile Trench. The anomaly along the northern margin of the Izu-Ogasawara Trench exceeds −200 mgal which is a largest one observed over the trenches of the surveyed area.

Rather high anomalies are observed midway along the frontal slope of the Tohoku and Kurile Axis. However, they are not found over all of the slope. Especially, the anomaly is not so apparent in the Kurile Trench, except in the southern margin.

Bouguer anomalies

The low free air gravity anomalies observed in the Cape Erimo area are calculated as approximately −110 mgal and −70 mgal Bouguer anomalies in the Hidaka Basin. The anomaly in to the east of Cape Erimo is calculated as approximately −120 mgal of the Bouguer anomaly. The water depth does not exceed 1,000 m in these areas, which are relatively shallower in comparison with the lower values of the anomalies. Therefore, it is suggested that the basins are filled by loose sediments.

High anomalies of 220 mgal are located southeast of Etorofu island which connect with the high anomalies of more than 140 mgal near the northeastern coast of Hokkaido.

High anomalies are observed along the Tohoku coastal region. The anomaly is approximately 160 mgal along the Sanriku coast and is approximately 140 mgal along the Abukuma coast.

References Cited

TALWANI, M., WORZEL, J. L. and LANDISMAN, M. (1959) Rapid gravity computations for two-dimensional bodies with application to the Mendocino submarine fracture zone. *Jour. Geophys. Res.*, vol. 64, p 49–59.

THE GEOGRAPHICAL SURVEY INSTITUTE (1955) *Gravity Survey in Japan* (1) I Gravity Survey in Hokkaido District. *Bull. Geographical Survey Institute*, vol. 4, part 2.